Journal of Thermal Analysis and Calorimetry, Vol. 93 (2008) 1, 281–287

DIELECTRIC CLASSIFICATION OF *D*- AND *L*-AMINO ACIDS BY THERMAL AND ANALYTICAL METHODS

M. E. Matthews, I. Atkinson, Lubaina Presswala, O. Najjar, Nadine Gerhardstein, R. Wei, Elizabeth Rye and A. T. Riga[*]

Department of Chemistry, Cleveland State University, Cleveland, Ohio 44115, USA

Dielectric analysis (DEA), supported by thermogravimetric analysis (TG), differential scanning calorimetry (DSC), powder X-ray diffraction analysis (PXRD) and photomicrography, reveal the chiral difference in the amino acids. The acids are classified as dielectric materials based on their structure, relating chirality to the vector sum of the average dipole moment, composed of the constant optical (electronic) and infra-red (atomic) polarizabilities, as well as dipole orientation. This study encompasses 14 *L*- and *D*-amino acid isomers. Physical properties recorded include AC electrical conductivity, charge transfer complexes, melting, recrystallization, amorphous and crystalline phases, and relaxation spectra, activation energies and polarization times for the electrical charging process.

Keywords: *activation energy, chiral recognition, dielectric analysis (DEA), dipole orientation, polarization*

Introduction

The key classification of all organic and biochemical compounds is the presence of at least one carbon atom in their molecular structure. This carbon atom, possessing four valence electrons, can bind with four different side groups or atoms, forming a tetrahedral structure. When the tetrahedral carbon atom in an organic molecule is connected to four differing groups, it is termed asymmetric or chiral. Molecules possessing a chiral carbon center are defined as chiral compounds, and their two isomers referred to as stereoisomers, two molecules of identical chemical structure but a different arrangement of their atoms in space.

Two enantiomers, non-superimposable mirror image forms, display identical physical and chemical properties except under a chiral influence, for example, in an optically polarized field. All amino acids with the exception of glycine exist in one or the other of two isomers, called the *L*- and *D*- isomers; only one isomeric form, *L*, displays activity in biological systems. Chiral compounds were first fully elucidated by Louis Pasteur in 1849 when he separated two different types of tartaric acid crystals in a racemic mixture and demonstrated that one rotated the plane of polarized light to the left, while the other rotated it to the right. Currently chiral compounds are studied, separated and even uniquely prepared or isolated using chiral stationary phases, chiral mediums, and sterioselective reactions [1]. Attempts at chiral recognition by thermal analysis have yielded mixed results; for example, a study of aqueous solutions of *D*-mannonaphtho-18-crown-6-ether 1 with *D*- and *L*-phenylalanine by microcalorimetry showed minimal chiral recognition [2].

We have classified the amino acids as dielectric materials based on their structure, relating chirality to the vector sum of the average dipole moment, which includes the constant optical (electronic) and infrared (atomic) polarizabilities. A third term, dipole orientation, completes the vector sum and validates the demonstrated ability to distinguish *D*- and *L*-amino acids by their dielectric behavior. The influence of the external dielectric field on the average dipole moment induced in a molecule can be separated as two types of contributions: (*i*) due to the elastic displacement of charges; and (*ii*) due to a change in the average orientation of the permanent dipole of the molecule. Thus, the average dipole moment (m) is composed of three related terms: the first two (m_0 and m_{ir}) are due to elastic displacements with proper frequencies in the optical and infrared regions; the third (m_d) is due to dipole orientation. Mathematically:

$$m=m_0+m_{ir}+m_d \quad (1)$$

Classification of dieletrics is accompanied by the division of polarizable materials into three types: (*i*) non-polar substances showing optical polarization only; (*ii*) polar substances having optical as well as infrared polarization; and (*iii*) dipolar substances which also show polarization due to dipole orientation, for

* Author for correspondence: a.riga@csuohio.edu

1388–6150/$20.00

Akadémiai Kiadó, Budapest, Hungary
Springer, Dordrecht, The Netherlands

example, the technique used in this study to differentiate chiral compounds [3].

The purpose of this research is to present evidence for a relationship between polarized dielectric analysis-conductivity and chiral structure in biological systems, specifically among *D*- and *L*-amino acids. Dielectric analysis (DEA), measuring frequency modulated conductivity and tan delta as a function of temperature, subjects a sample to an oscillating sinusoidal electric field whose applied voltage produces a polarization within the sample [4–6]. This technique was applied to a series of amino acid stereoisomers, to determine the chiral difference in the *D*- and *L*-amino acids. Thermogravimetric analysis (TG) and differential scanning calorimetry (DSC) support the DEA observations. Powder X-ray diffraction analysis (PXRD) and photomicrography of three sets of *D*- and *L*-amino acids, tryptophan, phenylalanine and lysine, further illustrated the differences. The physical properties recorded in this study include AC electrical conductivity (pS/cm) profiles, formation of charge transfer complexes, melting temperature/range, recrystallization, amorphous and crystalline phases, and relaxation spectra, activation energies and polarization times for the electrical charging process. The study encompasses 20 *L*-amino acids and the *D*-isomers of arginine, cysteine, glutamic acid, lysine, phenylalanine and tryptophan. The electrical conductivity of the *L*-amino acids generally exceeded that of their *D*-isomer at 150°C with an applied frequency of 1000 Hz (bulk analysis) and 1.00 Hz (surface analysis). Comparisons within each isomer group (*L*- to *L*-; *D*- to *D*-) indicated electrical conductivity of the samples also correlated with moisture content and amorphous–crystalline composition [7].

Experimental

The employment of DEA, in conjunction with supporting DSC and TG, provides a rich, multi-layered understanding of amino acid behavior. For DEA, a sample was placed on a single surface gold ceramic interdigitated electrode. An applied sinusoidal voltage creates an alternating electric field, producing polarization in the sample which oscillates at the same frequency as the electric field. However, there is a phase angle shift measured by comparing the applied voltage to the measured current. The current is then separated into capacitive (*e*') and conductive (*e*") components. Permittivity (*e*') is proportional to the capacitance and measures the number of dipoles. The loss factor (*e*") is proportional to the conductance and represents the energy required to align dipoles and move ions. Ionic conductivity relates to the viscosity of the sample because fluidity is identified by the ease with which ionic components can migrate through the sample under the applied electric field [8, 9].

DEA measures the electrical properties, in our study, of crystalline amino acids, as a function of time, temperature, and frequency. Two fundamental characteristics are measured by dielectrics. First, the capacitive nature of the amino acids allows these materials to store electrical charge. Second, the conductivity characteristic represents the ability of the amino acid to transfer electrical charge. These properties are significant since they have been correlated to an action on a molecular level, the variation of the conductivity in the pre-melt of the amino acids studied. This technique has the capability to explore the rheology and molecular mobility of the amino acids 20 to 30°C below the melting point established by DSC.

The amino acids studied were the *D*- and *L*-isomers of arginine, cysteine, glutamic acid, lysine, phenylalanine and tryptophan. These crystalline amino acids were obtained from Sigma-Aldrich (St. Louis, Mo.). Experimental conditions for all procedures were standardized to eliminate environmental factors from influencing the analyses.

PXRD were performed using a one piece, Bakelite well mount and a Bragg–Brentano configuration. Samples were examined from 5 to 60° 2θ. The values were obtained at a scan rate of 2° 2θ min^{-1}. d-spacing values (Å) and the correlating relative intensities were generated for each sample.

An Olympus BX60 microscope and camera were used to capture black and white photographic images of three pairs of *D*- and *L*-amino acids at 10× optical and 40× objective lens magnification.

A TA Instruments (TAI) 2970 DEA was used to determine the electrical conductivity profile of the amino acids. For each amino acid, a sample of approximately 10 mg was placed on a single surface gold ceramic interdigitated electrode in an isolated nitrogen rich dry atmosphere. The samples were ramped at a rate of 10°C min^{-1} from room temperature (24°C) to just above melting. Conductivity measurements were recorded at controlled interval frequencies ranging from 0.10 to 10,000 Hz for all temperatures.

A TAI 2920 DSC was used to characterize melting, and crystallization properties of the samples. Aluminum pans and lids were prepared with samples weighing between 7 and 14 mg and subjected to a cool and heat series cycling between –50 and 150°C at a rate of 10°C min^{-1} in an isolated nitrogen atmosphere. Heat flow (W g^{-1}) values *vs.* time and temperature were generated.

A TAI 2950 TGA was used to measure the percent mass loss of the amino acids when heated to temperatures below the melting point, but above the

boiling point of water. Samples were loaded into aluminum pans and heated in an isolated nitrogen environment to 150°C. Isothermal conditions were then maintained to ensure reaction completion.

Results and discussion

Dieletric analysis: conductivity

DEA profiles of the amino acids studied show the *L*-isomer is consistently more conducting than its *D*-counterpart (Table 1). This trend is best illustrated by comparing conductivity of *L*- and *D*-forms at a given temperature and frequency. Lower frequencies of 1.00 Hz or less reveal surface reactions; frequencies at or above 1000 Hz reveal bulk reactions. For this reason, the points of comparison used in this study were taken from the 1.00 and 1000 Hz frequencies.

Melting points of the amino acids range from 225 to 290°C; to capture the acids in a variety of phases, points of DEA comparison were taken at 115°C, well below the observed melting points; 150°C, below the melting point but in the linear pre-melt region for most amino acids; and 225°C, at melting or in the pre-melt region for all amino acids.

These parameters yield six data points for each isomer: conductivity at 1.00 Hz and 115, 150 and 225°C; and conductivity at 1000 Hz and 115, 150 and 225°C. In each *D*- and *L*-pairing, these points indicated the *L*-isomer was more conducting across the range of frequencies and temperatures. In the six cases where *D*-isomer was more conducting than *L*-species, two show a ratio of 0.9; accounting for experimental error, these ratios indicate *D*- and *L*- are roughly equivalent. All six cases occur at 115°C, the lowest temperature examined. Conductivity at 115°C, below the melting point, may be affected by factors outside stereochemistry, such as the percent amorphous character of the samples and their initial moisture content.

Although the *L*-isomers' conductivity consistently exceeded that of the *D*-isomers, the ratio varied greatly depending on temperature and frequency. At the high end of the spectrum, *L*-cysteine was 52.000% more conducting than *D*-cysteine at 1.00 Hz and 150°C. At the other end of the spectrum, *L*-lysine is 13% more conducting than *D*-lysine at 1.00 Hz and 150°C. A ratio so close to one does not show a strong conductivity advantage to either *L*- or *D*- on its own, but it supports the trend of the series of data points showing *L*-isomers consistently more conducting than *D*-forms. Conductivity profiles of lysine provide a good illustration of this trend, with the *L*-isomer more conducting than *D* at all temperatures at 1.00 and 1000 Hz (Fig. 1). However, examination by DEA of the cooled melted amino acid, for example, lysine, from room temperature to 225°C showed for all temperatures that the *D*-lysine was significantly more conducting that the *L*-lysine (Fig. 2). This observation is attributed to the higher amorphous content in the *D*-isomer. We have observed for 14 drugs (active pharmaceutical ingredients) the crystalline phase to be statistically much less conducting (e.g. 10^{-2} pS cm^{-1}) and the amorphous phase more conducting (e.g. 10^{+6} pS cm^{-1}) [10].

Table 1 Conductivity: *L vs*. *D*/(%)

Sample	1 Hz		1000 Hz	
	150°C	225°C	150°C	225°C
Arginine	21	2455	211	11646
Cysteine	52346	30	14112	10
Glutamic acid	16	no data	117	190
Lysine	13	470	–3	30
Phenyl-alanine	32	1172	128	101
Tryptophan	379	56	925	244

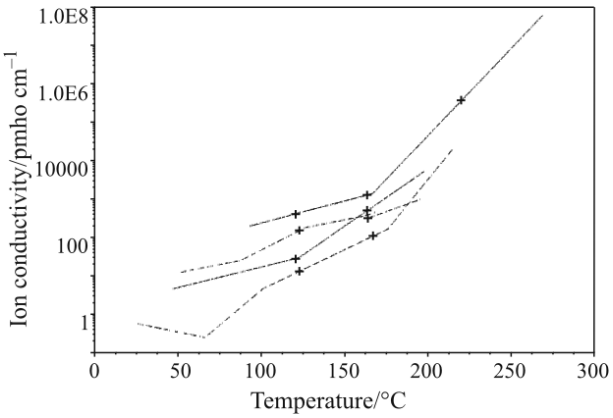

Fig. 1 - - - - – *D*- and —— – *L*-lysine conductivity profiles at 1.00 and 1000 Hz

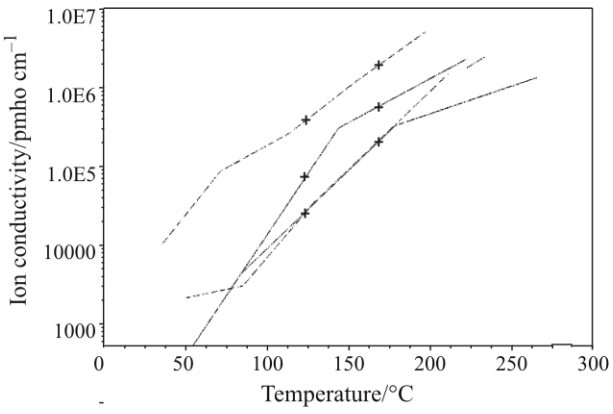

Fig. 2 Melted and cooled - - - - – *D*- and —— – *L*-lysine conductivity profiles at 1.00 and 1000 Hz

Pre-melt Arrhenius plots of log conductivity vs. 1/T: activation energies

It has been observed that some chemicals form thermally-induced excimers or charge-transfer complexes prior to melting in the solid state. DEA conductivity profiles show this phenomenon as a sharply linear increase in conductivity leading into the melt identified by DSC (R^2 of 0.999). Previous studies of melting behavior in drugs show a corresponding softening of the material over the same temperature range measured by thermal mechanical analysis (TMA). These visco-elastic dielectric transition temperatures, identified by DEA and TMA, bracket the chemical and mechanical changes the material undergoes as it moves from solid to liquid. Frequency-dependent activation energies based on the linear pre-melt region of the DEA profiles were calculated for several pairs of *D*- and *L*-amino acids, including lysine, arginine and phenylalanine. Arrhenius plots of log conductivity *vs*. the inverse temperature in K yielded linear curves with R^2 values between 0.99 and 1.0. Activation energies calculated from the slope of these curves taken at a frequency of 1.00 Hz ranged from approximately 100 to 500 J, with the majority falling between 100 and 200 J. Additionally, activation energies for the *L*-isomers consistently exceeded that of the *D*-isomers.

To place these activation energies in context, a study of anthracene and eight drugs or excipients (vanillin, sulfapyridine, lidocaine, tolbutamide, caffeine, acetanilide, acetopheneditin and nifedipine) yielded activation energies from 60 J (lidocaine) to 1600 J (acetopheneditin) at 1.00 Hz. Vanillin and caffeine measured 250 and 300 J, respectively, while the rest fell closer to 1100 J [10].

Arrhenius plots of log(tanδ) vs. 1/T: relaxation spectra and polarization times

A subset of the amino acids studied produced relaxation spectra in plots of DEA-generated tanδ *vs*. temperature and frequency. These spectra, a series of regular peaks, indicate an ordered charging-discharging process in the material. Spectra observed in *L*-lysine and *L*-arginine were analyzed to obtain activation energies (for the charging-discharging process, separate from the pre-melt activation energies previously discussed), frequency factors and polarization times. Examinations of cytochrome C, a protein and known charge carrier in the electron transport chain, show the activation energy to be around 70 J.

Polarization times for *L*-lysine and *L*-arginine ranged from $2\cdot10^{-7}$ to $2\cdot10^{-4}$ s, depending on temperature. For a point of comparison, a study of benzophenone in benzene observed polarization times of 10^{-11} s [11].

Table 2 Pre-melt activation energies at 1.00 Hz

Sample	E_a/J	R^2	Temp. range/°C	T_m/°C
L-Lysine	194	0.99	224–238	224
D-Lysine	127	1.00	216–226	224
L-Arginine	144	0.99	228–238	244
D-Arginine	135	0.99	228–238	244
L-Phenylalanine	533	1.00	276–288	283
D-Phenylalanine	117	0.99	258–274	285

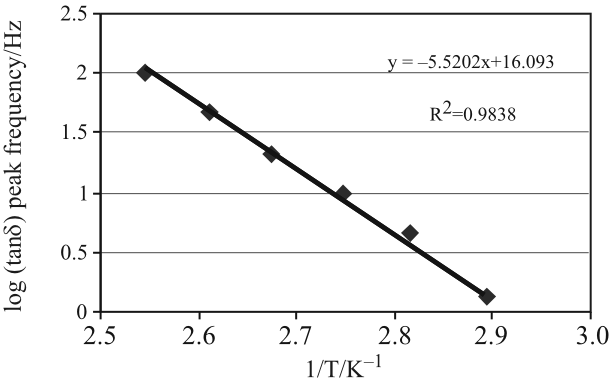

Fig. 3 *L*-lysine activation energy

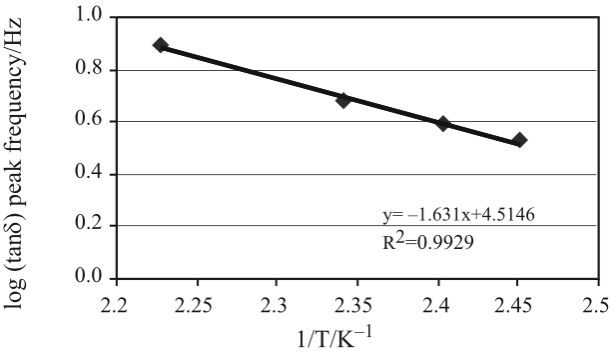

Fig. 4 *L*-arginine activation energy

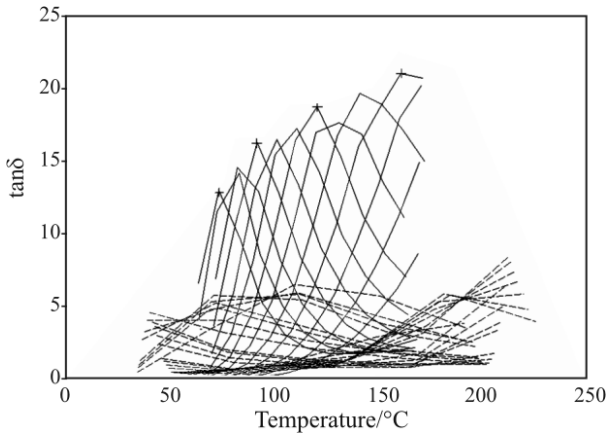

Fig. 5 - - - - – *D*- and —— – *L*-lysine relaxation spectra

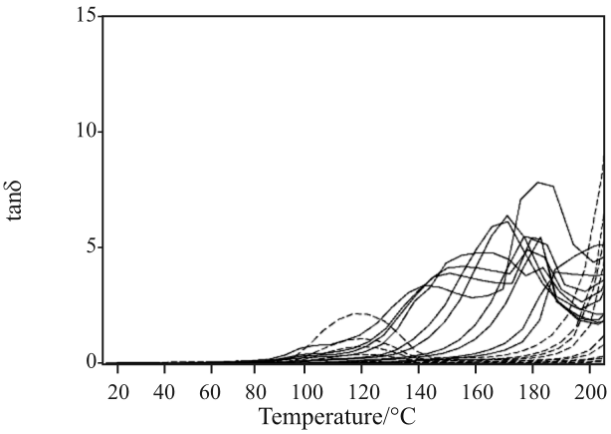

Fig. 6 - - - - – *D*- and — – *L*-arginine relaxation spectra

For a given polarization time, *L*-lysine requires a lower temperature threshold than *L*-arginine; this also relates to the frequency factors, describing the number of collisions per second, 10^{16} for *L*-lysine *vs*. 10^4 for *L*-arginine. Figures 5 and 6 above give a visual representation of these numbers: the peaks for *L*-lysine are sharp, tightly packed, and regularly spaced – thus, the material polarizes quickly with high frequency. *L*-arginine's broad, diffuse peaks indicate a slower, less regular charging/discharging.

Table 3 Relaxation spectra

Sample	E_a /J	Freq. factor/s^{-1}
L-Lysine	106	1.24E+16
L-Arginine	31	3.27E+04
Cytochrome C	71	4.99E+09

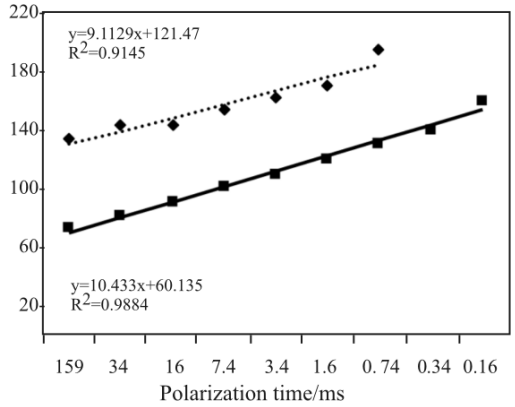

Fig. 7 Polarization times for — – *L*-lysine and ····· – *L*-arginine

PXRD and photomicrography

L- and *D*-lysine were examined by PXRD. *D*-lysine had a full complement of interplanar distances and intensities. *L*-lysine had a number of similar diffraction spacings, however, there were major differences, including a number of spacings present in *D*-lysine and absent in *L*-lysine: for example, the spacings at 17.3, 4.9, 4.8, 4.7 and 3.7 Å with relative intensities from 43 to 65%, major structural features. The *D*-isomer had an absent line at 4.5 Å (38% relative intensity).

Table 4 Lysine PXRD

D-spacing		Relative intensity	
D	*L*	*D*	*L*
17.3		65	
10.5	10.6	10	18
10.2		8	
4.9		43	
4.8		57	
4.7		58	
4.6	4.6	89	33
4.5	4.5	97	42
	4.5		38
4.4	4.2	100	67
4.2	4.2	93	63
3.7		44	
3.5	3.5	66	100
3.3		27	
3.1	3.1	29	43

Optical photomicrography of *D*- and *L*-lysine taken at a magnification of 40× revealed two interesting features. First, lysine is hygroscopic and the pictures were recorded in a room with relative humidity of 60% or greater. The crystalline solids reacted with the atmospheric moisture, dispersing islands of crystals within water droplets. However, the crystal morphology of the *D*-form exhibited small, evenly dispersed aggregate clusters in small streams of water while the *L*-isomer formed islands of water containing larger aggregates of crystals. Prior to exposure to the atmospheric moisture, the *D*-crystals were observed to be smaller and finer than the *L*-form.

PXRD of *D*- and *L*-tryptophan, a more hydrophobic amino acid, revealed a significant difference at 6.0 Å, absent from the *L*-form and at 100% relative intensity in the *D*-form. An additional spacing at 4.7 Å (13%)

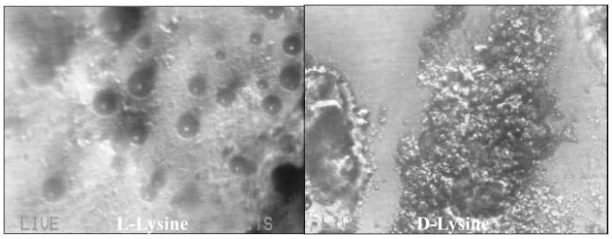

Fig. 8 Lysine photomicrography

Table 5 Tryptophan PXRD

D-spacing		Relative intensity	
D	*L*	*D*	*L*
6.2	6.1	93	10
6.0		100	
4.8	4.9	30	55
	4.7		13
4.6	4.6	50	44
4.0	4.1	52	43
3.8	3.9	37	77
3.7	3.8	28	59

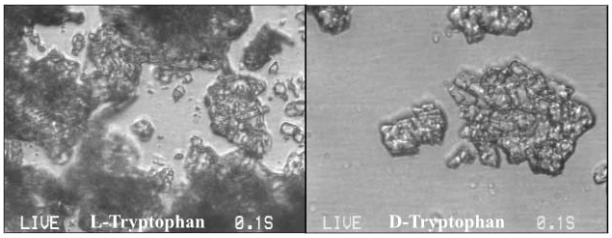

Fig. 9 Tryptophan photomicrography

was present in *L*- and absent in *D*-. However, the overall structures of the two isomers remain similar.

Photomicrography at 10× optical and 40× objective magnification shows the similarities in crystal structure. *D*-tryptophan's crystals appear in smaller, more ordered clusters, but the overall appearance of sharp, flat lines is the same in both isomers.

A third PXRD analysis of *D*- and *L*-phenylalanine showed the *D*-phenylalanine XRD pattern was very similar to the *L*-isomer XRD pattern with little or no significant differences. Photomicrography confirmed the crystal morphology to be similar.

Additionally, a major interplanar distance – relative intensities between 50 and 100% – was observed for the six amino acids at 4.0 to 4.2 Å. This implies that there is a common structural feature at this distance.

Table 6 Phenylalanine PXRD

D-spacing		Relative intensity	
D	*L*	*D*	*L*
17.4	17.3	3	2
16.4		11	
8.2	8.2	1	1
5.4	5.4	21	24
5.1	5.1	3	9
4.0	4.0	100	100
3.2	3.2	44	39
2.7	2.7	40	35

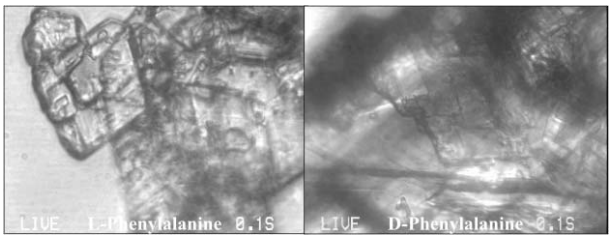

Fig. 10 Phenylalanine photomicrography

Conclusions

Employing DEA as an analytical technique, we have distinguished the unique dipole characteristics of chiral molecules, specifically *D*- and *L*-amino acids. These preliminary, repeatable results indicate a potential expansion of the technique to distinguish a host of chiral molecules. In addition to chiral detection, we are able to make several general statements about the electrical behavior and structural features of the amino acids studied:

- *L*-isomers are generally more conducting than their *D*-counterparts at a given temperature and frequency.
- After melting, the cooled *D*-isomers generally become more conducting than their *L*-counterparts. This indicates the *D*-forms may be more amorphous in the liquid phase.
- Sharply linear pre-melt conductivity increases were used to calculate activation energies, similar in magnitude to those observed for caffeine and vanillin.
- Polarization spectra observed for *L*-lysine, *L*-arginine and cytochrome C indicate the presence of a charging–discharging process. These spectra were used to calculate activation energies, frequency factors and polarization times.
- Explorations of morphology and crystal structure via PXRD and photomicrography parallel the DEA results, showing a significant difference between *D*- and *L*-lysine, some differences in *D*- and *L*-tryptophan and little or no difference in *D*- and *L*-phenylalanine.

References

1 M. G. Finn, Chirality, 14 (2002) 534.
2 M. Koźbiał, J. Poznański, E. Utzig and J. Lipkowski, J. Therm. Anal. Cal., 83 (2006) 575.
3 H. Frohlich, Theory of Dieletrics: Dieletric Constant and Dieletric Loss, Oxford Science Publications, Oxford 1986, pp. 104–121.
4 P. J. Haines Ed., Principles of Thermal Analysis and Calorimetry, RSC Paperbacks, Cambridge 2002, p. 99.

5 J. Cahoon, A. Riga and V. Lvovich, Materials Characterization by Dynamic and Modulated Thermal Analytical Techniques, ASTM STP 1402, American Society for Testing and Materials, West Conshohocken, PA 2001, pp. 157–173.
6 A. Riga, J. Cahoon and J. W. Pialet, Materials Characterization by Dynamic and Modulated Thermal Analytical Techniques, ASTM STP 1402, American Society for Testing and Materials, West Conshohocken, PA 2001, pp. 139–156.
7 L. Presswala, M. E. Matthews, I. Atkinson, O. Najjar, N. Gerhardstein, J. Moran, R. Wei and A. Riga, Hydration of Crystalline Amino Acids with Bound and Unbound Water Revealed by Thermal Analysis, NATAS Conference, August 2007, Lansing, Michigan.
8 Netzsch Instruments, Inc., 37 North Ave., Burlington, MA 01803
9 TA Instruments, 109 Lukens Drive, New Castle, DE 19720
10 A. Riga and K. Alexander, Amer. Pharm. Rev., 6 (45) (2005) 50.
11 H. Frohlich, Theory of Dieletrics: Dieletric Constant and Dieletric Loss, Oxford Science Publications, Oxford 1986, p. 122.

DOI: 10.1007/s10973-007-8835-8